Supplementary Information Appendix for

Neurons Differentiate Magnitude and Location of Mechanical Stimuli

Benjamin M. Gaub[a,1,2], Krishna Chaitanya Kasuba[a,1], Emilie Mace[b], Tobias Strittmatter[a], Pawel R. Laskowski[a], Sydney A. Geissler[a], Andreas Hierlemann[a], Martin Fussenegger[a], Botond Roska[b] and Daniel J. Müller[a,2]

[a] Eidgenössische Technische Hochschule (ETH) Zurich, Department of Biosystems Science and Engineering, Mattenstrasse 26, 4058 Basel, Switzerland.

[b] Friedrich Miescher Institute for Biomedical Research (FMI), Neural Circuit Laboratories, Maulbeerstrasse 66, 4058 Basel, Switzerland.

[1] B.M.G. and K.C.K. contributed equally to this work.

[2] Correspondence: benjamin.gaub@bsse.ethz.ch and daniel.mueller@bsse.ethz.ch

This PDF file includes:

Supplementary Figure S10. Logistic regression comparing the effect of various chemical compounds to neuronal responses evoked by shear stress.

Supplementary Figure S11. Mechanical properties of neuronal compartments.

Supplementary Table S1. mRNA transcript levels of ion channels in E18 and adult cortical rat neurons.

Supplementary References

Other supplementary materials for this manuscript include the following:

Supplementary Video S1. Ensemble of neurons responding to shear stress.

Supplementary Video S2. Transient neuronal response to soma stimulation.

Supplementary Video S3. Sustained neuronal response to soma stimulation.

Supplementary Video S4. Global neuronal response to axon stimulation.

Supplementary Video S5. Local neuronal response to dendrite stimulation.

Supplementary Text

Text S1. Conversion of force values to pressure values.

To compare the force-threshold values with published pressure values, we calculated the pressure resulting from mechanical stimulations pushing a 5 μm diameter bead onto the soma. The contact area *A* between bead and soma is given as half sphere surface of the bead:

$$A = 2\pi\, r^2 \qquad \text{Equation S1}$$

with *r* = 2.5 μm, the area *A* is:

$$A = 2\pi(2.5\ \mu\text{m})^2 = 39.3\ \mu m^2$$

The pressure *P* is given as:

$$P = \frac{F}{A} \qquad \text{Equation S2}$$

with *F* being the indentation force. The pressure *P* corresponding to the indentation force were calculated the following way: For an indenting force of 100 nN, *P* is:

$$P = \frac{100 * 10^{-9}\ \text{kg m s}^{-2}}{39.3 * 10^{-12}\ m^2} = 2.55 * 10^3 \text{kg m}^{-1}\ \text{s}^{-2} = 2.55\ kPa$$

Using this formula, we obtain the following pressure values for given forces:

200 nN = 5.1 kPa;

300 nN = 7.6 kPa;

400 nN = 10.2 kPa;

265.5 nN = 6.8 kPa;

285 nN = 7.3 kPa;

230 nN = 5.6 kPa;

330 nN = 8.4 kPa;

370 nN = 9.4 kPa

Text S2. Estimation of pressure applied to axons and dendrites upon indenting beads by AFM.

To estimate the pressure applied to axons and dendrites upon locally indentation by AFM, we considered the indenter to be a mono-disperse silica bead (sphere) of 5 µm diameter (**Materials and Methods, SI Appendix, Text S2 Fig. S1**). In order to estimate the contact area, we assume the neuronal processes to be flattened upon mechanical compression with the bead (**SI Appendix, Text S2 Fig. S1B**). The maximum contact area *A* between the indenting bead and the indented axon/dendrite can be described by a bead (sphere) of radius r_B pushing onto the neuronal process (estimated as elongated cylinder) having a diameter d_p as shown below. Upon compression the cylindrical process flattens and the contact area between bead and axon/dendrite increases.

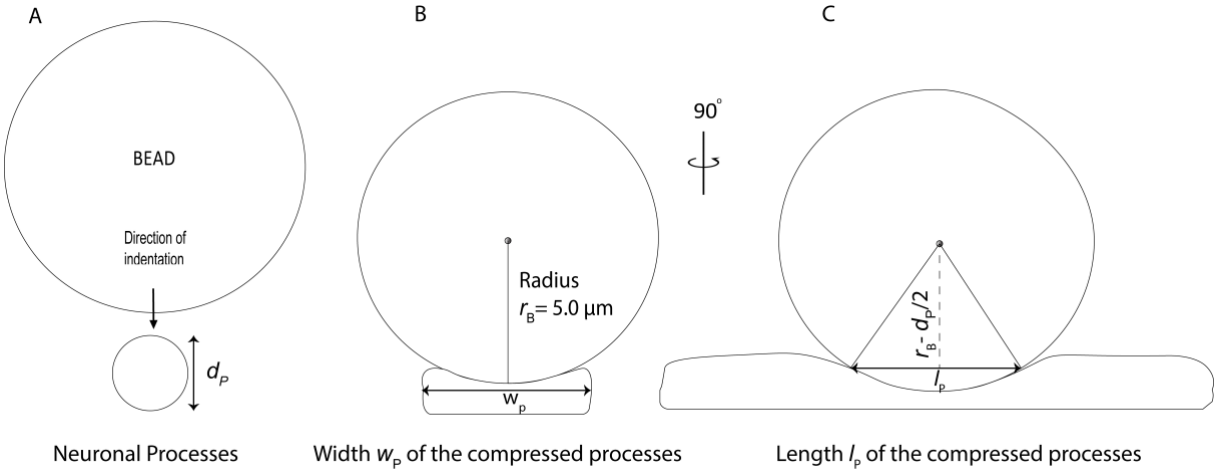

Text S2 Fig. S1. Estimation of the maximum contact area between a micrometer sized bead indenting a neuronal processes such as axon or dendrite. (A), In our experiment a micrometer-sized bead presses onto the neuronal process, an axon or dendrite, which is here described by a soft cylinder having a diameter d_P. Average d_P values are measured by super-resolution microscopy (see below). (B), By applying sufficiently high forces the soft cylinder flattens, which increases the contact area *A* between bead and axon/dendrite. The contact area can be estimated by the bead radius r_B, the length of the compression applied to axon/dendrite l_P, and the width of the compressed axon/dendrite w_P. **c**, Longitudinal view along the cylinder compressed by the bead, with l_P indicated. l_P can be estimated by the cord of the bead at distance $r_B - d_P/2$ from the center of the bead.

The contact area *A* between bead and axon or dendrite can be calculated from:

1) The bead radius r_B = 5.0 µm
2) The diameter d_P of the uncompressed process, axon or dendrite, as estimated by super-resolution microscopy (**SI Appendix, Fig. S7**)
3) The width of the compressed axon/dendrite w_P, which is roughly estimated to be half of the circumference of the uncompressed axon/dendrite, $d_P*\pi/2$
4) The length of compressed axon/dendrite l_P, which can be estimated by the cord of the bead at distance $r_B - d_P/2$ from the centre of the bead
   $l_P \approx (2*(r_{B2} - (r_B - d_P/2)_2))_{0.5}$

Average contact area of bead and axon:

Average diameter of axon d_P = 0.83 ± 0.07 µm (ave ± SEM, as determined by STED microscopy)
Indentation depth $d_P/2 \approx$ 0.42 ± 0.04 µm
Length of compressed axon $l_P \approx$ 4.10 ± 0.28 µm
Width of compressed axon $w_P \approx$ 1.32 ± 0.13 µm
Average contact area *A* of axon

= l_P x w_P ≈ 4.10 ± 0.28 µm x 1.32 ± 0.13 µm
≈ 5.42 ± 0.87 µm^2

Average contact area of bead and dendrite:
Average diameter of dendrite d_P = 1.43 ± 0.18 µm (ave ± SEM, as determined by STED microscopy)
Indentation depth = $d_P/2$ ≈ 0.72 ± 0.09 µm
Length of compressed dendrite l_P ≈ 5.14 ± 0.32 µm
Width of compressed dendrite w_P ≈ 2.26 ± 0.28 µm
Average contact area A of dendrite
= l_P x w_P ≈ 5.14 ± 0.32 µm x 2.26 ± 0.28 µm
≈ 11.61 ± 0.99 µm^2

The pressure P is given as:

$$P = \frac{F}{A} \qquad \text{Equation S2}$$

with F being the indentation force. For an applied force of ≈ 230 nN, the corresponding P applied to axon and dendrite can thus be approximated as:

For axons: $P \approx \frac{230*10^{-9}\ \mathrm{kg\ m\ s^{-2}}}{5.42*10^{-12}\ m^2} \approx 65.7 * 10^3\ \mathrm{kg\ m^{-1}\ s^{-2}} \approx 42.44 \pm 8.14\ kPa$

For dendrites: $P \approx \frac{230*10^{-9}\ \mathrm{kg\ m\ s^{-2}}}{11.61*10^{-12}\ m^2} \approx 30.06 * 10^3\ \mathrm{kg\ m^{-1}\ s^{-2}} \approx 19.81 \pm 1.61\ kPa$

Supplementary Methods

Neuron culture. Neurons were cultured following a standard protocol (1). Briefly, E18 Wistar rats were sacrificed, and cortices and hippocampi were removed and dissociated using trypsin with 0.25% EDTA (Thermo Fisher Scientific, Reinach, Switzerland) followed by physical trituration. All animal protocols were approved by the Basel Stadt veterinary office according to Swiss federal laws on animal welfare. Glass coverslips were washed 3x with sterile water and coated with 50 µl of 0.05% polyethyleneimine (Sigma, Buchs, Switzerland) in borate buffer (Chemie Brunschwig, Basel, Switzerland) for 1 h at room temperature (RT). After primary coating, coverslips were washed 3x with water and dried thoroughly. For secondary coating a 20 µl drop of laminin (Sigma) at 0.02 mg ml_{-1} in neurobasal medium (Thermo Fisher Scientific) was deposited in the center of the coverslip and incubated for 30 min at 37°C and 99% humidity. Then, ≈ 50,000 cells were seeded onto the coverslip and the cells were allowed to attach for 30 min before adding 1 ml of neurobasal medium. Cultures were maintained inside an incubator under controlled environmental conditions (37°C and 5% CO_2) and half of the neurobasal medium supplemented with 0.5 mM GlutaMAX and 2% B27 (Thermo Fisher Scientific) was exchanged every 3 days.

Combined shear stress and widefield microscopy. Mechanical stimulation of neurons by shear stress was performed using a custom-built piston array which was inspired by a recent study (2). Briefly, a 96-piston array was 3D printed by Protolabs (Feldkirchen, Germany) using ABS black resin (SL7820, 3D Systems). Each piston had a circular face with a diameter of 5.4 mm. The piston array was attached to a loudspeaker (W3-1750S, TB speakers) which actuated the piston array vertically. To precisely monitor the output of the pistons, we integrated an accelerometer (ADXL337, Analog Devices, MA, USA) and displayed the signal using an oscilloscope. The assembly sits on a machined aluminum assay plate guide which is designed for a standard 96-well plate. A signal generator (DS345, Stanford Research Systems, Lausanne, Switzerland) was used to generate a low frequency (60 Hz) sign wave, which was amplified using an amplifier (SPL400, Skytec, Twente, Netherlands). This amplified signal was used to drive the speaker and actuate the piston array. The frequency of the signal was set on the signal generator; the amplitude was set on the amplifier. The piston device was mounted on a widefield microscope (Nikon Eclipse Ti, Nikon GmbH, Düsseldorf, Germany) equipped with a 10X air objective (Nikon Plan Flour 10x/0.3), an illumination system (SpectraX7, Lumencor, OR, USA) and an environmental chamber for CO_2 and temperature control. Time lapse images were acquired using 488 nm excitation and 100 ms exposure.

Two stimulation protocols were used for mechanical stimulation of neurons by shear stress. First, to characterize fundamental aspects of population and single cell response of cortical neurons (**Fig. 1**), we delivered a single stimulus (3 s duration, 60 Hz oscillation and ≈ 4 mm piston amplitude) and imaged neurons during the stimulus to determine the response and for 1 min before and after the stimulus to determine spontaneous activity, unless otherwise noted. Second, to assess the effect of chemical inhibitors (**Fig. 5**), neurons first received one pre-stimulus and after 57 s of rest another stimulus of 3 s duration, at 60 Hz and ≈ 4 mm amplitude. The responses to the first stimulus (pre-stimulus) was always stronger than consecutive stimuli so we decided to discard the pre-stimulus and start with second stimulus. The device was opened and the compound was added to the well of interest by pipette as concentrated stock solution with minimal volume (≈ 1 – 5 µl). The compound was immediately mixed with the buffer in the well using a quick actuation of the pistons (1-s duration at 60 Hz

and ≈ 4 mm amplitude) and allowed 1 min of rest before another stimulus was delivered (3-s duration at 60 Hz and ≈ 4 mm amplitude). To avoid carry over of the compound, pistons were washed with water and ethanol and dried before moving to the next 96-well plate. Following published procedures (2, 3), we estimated the pressure applied in our shear stress experiments to ranging from ≈ 1 – 5 Pa.

Combined atomic force microscopy (AFM) and confocal microscopy. Confocal imaging was performed using an inverted laser-scanning confocal microscope (Observer Z1, LSM 700, Zeiss, Oberkochen, Germany) equipped with a 25x/0.8 LCI PlanApo water immersion objective (Zeiss). To ensure optimal recording conditions, we used an environmentally controlled chamber with constant CO_2 and temperature control (4). In addition, we heated the entire AFM and confocal microscope to 35°C using a space heater to prevent temperature gradients within the chamber. Lasers and channels were assigned using the "best signal" option to ensure that there was no spectral overlap between them. GCAMP expressing cells were located and regions of interest around probed cells were assigned to maximize the acquisition speed. Time-lapse images were acquired with 100 – 300 ms time resolution. Time-lapse imaging was initiated > 10 s before the onset of the mechanical stimulus. An AFM (CellHesion 200, JPK Instruments, Berlin, Germany) was mounted onto the confocal microscope. 5 µm diameter silica beads (Kisker Biotech) were glued to the free end of tipless microcantilevers (CSC-37, Micromash HQ, Sofia, Bulgaria) using UV glue (Dymax, CT, USA) and cured under UV light for 20 min. Cantilevers with beads were plasma-treated for 5 min using a plasma cleaner (Harrick Plasma, NY, USA) to ensure a clean surface and mounted on a standard glass cantilever holder (JPK Instruments) of the AFM. Cantilevers were calibrated using the thermal noise method (5). Mechanical stimulation protocols were programmed using the JPK CellHesion software. For mechanical stimulation, the AFM lowered the bead on the cantilever onto the cell with a speed of 10 µm s^{-1} until the force reached the set point, held the set point force at constant force for 250 ms, and then retracted with a speed of 100 µm s^{-1}. Set point forces were applied in intervals from 100 to 400 nN with 50 nN increments and within time intervals ranging from 10 – 20 s until a response was recorded. After each response, the cantilever was retracted, and a new neuron was stimulated with the exception of one experiment (**Fig. 3C**) in which we recorded serial responses of the same neuron. The percentage of neurons showing responses to mechanical stimulation varied between 50 – 96%, which may be attributed to age, health, density and quality of the neuronal preparation. All data for figure panels were taken from experiments from one neuronal preparation for consistency. To mechanoporate the membrane of neurons (**SI Appendix, Fig. S5C**), we used cantilevers with a sharp conical tip of a nominal radius of 35 nm and a nominal spring constant of 1 N m^{-1} (MESP, Bruker, Karlsruhe, Germany) and applied forces ranging from 50 – 350 nN.

Chemical reagents. For AFM experiments, glutamate receptor antagonists DNQX (10 µM in 0.1% DMSO, 99.9% neurobasal medium, Tocris, Zug, Switzerland) and D/L AP-5 (40 µM in 0.4% H_2O, 99.6% neurobasal medium, Tocris) were added to the neurobasal medium before mechanical stimulation to block spontaneous activity and isolate evoked mechanical responses. Piston experiments were performed without DNQX or D/L AP-5. In AFM and piston experiments, application of the vehicle alone (1% DMSO) had no effect on the force thresholds or magnitude of neuronal responses (**Fig. 5A, SI Appendix, Fig. S2A**). Chemical inhibitors were sourced from the following suppliers and applied in AFM and piston experiments at the following working concentrations: BAPTA (2mM, Enzo Life Sciences, Lorrach, Germany), GsMTx4

(2.5 µM, Tocris), 2-APB (100 µM, Tocris), TTX (1 µM, Tocris), benipidine (1 µM, Tocris), gadolinium chloride (100 µM, Tocris), ruthenium red (100 µM, Sigma), TRPV4/TRPV1 inhibitor capsazepine (2.5 µM), TRPV4 inhibitor RN1734 (5 µM, Tocris), and TRPV1 inhibitor AMG9810 (0.1 µM, Tocris). For piston experiments, the identical set of neurons was compared before and after application of the compound. Neurons were incubated for 20 min with inhibitors before mechanical stimulation. Efficacy was tested by comparing mechanically evoked responses of 10 neurons pre- and post-application of inhibitors. For experiments testing plasma membrane integrity (**SI Appendix, Fig. S5**), 10 µM propidium iodide (PI, Sigma Aldrich) was added to the neurobasal medium. For each chemical inhibitor characterized by AFM, we recorded a reference calcium signal of ≈ 10 neurons.

Functional calcium imaging analysis of piston experiments. A custom Matlab code was used to identify cells and plot their fluorescence traces over time. For every time point, candidate cells were segmented by applying a Laplacian of Gaussian filter (sigma = 25 pixels) on the raw fluorescence image and finding local maxima. Position and intensity for every candidate cell at every time point were saved. The median intensity of all candidate cells over time was calculated and used to find the maximum intensity of the time series and its corresponding time point t_{max}. Cells were selected for further analysis if their fluorescence intensity I at t_{max} was greater than a threshold value, defined (I > mm +T*mad) where mm is the median intensity of all candidate cells at t_{max}, mad the median absolute variation of all candidate cells and T a threshold factor adjusted for each analysis. For all chemical inhibition experiments (**Fig. 5**), the threshold factor was kept constant for “pre” and “post” conditions. Intensity over time (averaged over a 3x3 pixels area) was saved for all selected cells. Normalized GCaMP fluorescence values $\Delta I/I$ were calculated for each cell using $\Delta I/I = (I_{max} – I_{ave}) / I_{ave}$., with I_{max} being the peak fluorescence intensity value at t_{max} and I_{ave} the average fluorescence intensity value preceding the stimulation. All cells with responses of $\Delta I/I > 0.1$ were counted as “responders” and further analysed. To examine the dynamics of the neuronal response, we looked at the average responses of all cells. We analyzed a total of 2880 cortex neurons from 21 experiments out which 2731 cells responded = 94.8%. We analyzed a total of 298 hippocampal neurons from 7 experiments out which 298 neurons responded = 100%. We calculated the decay times (for time periods of 20% to 90% of the peak amplitude) which were on average 1.4 s. We classified responses as transient if they were < 2.8 s and as sustained if they were > 2.8 s.

Functional calcium imaging analysis of AFM experiments. For each recording, an average calcium signal curve $\Delta I/I$ was calculated as the mean signal over the entire image relative to the first time point of the curve. For recordings with multiple AFM stimulations, peaks were detected from the curve as events with minimal amplitude of 0.25 and minimal time interval between peaks of 1 s. For each event, the start of the response was determined as the time point when the calcium signal amplitude crossed 20% of the peak value. Data from 2.5 s before and 5 s after the start of the response peak (t = 0) was plotted. Rise time of the response was calculated as the time to reach from 20% to 90% of the peak. To cluster responses, all single responses were first normalized to the peak value. Normalized responses were clustered using k_{means} algorithm (Matlab function k_{means}, using square Euclidean distance). The optimal number of clusters was evaluated using the silhouette function. Activity heat maps of calcium data (**Fig. 2C**) were computed as the relative difference between the average image for the 1 s following peak compared to the average image during the first 1 s of the recording (baseline). Only pixels with $\Delta I/I > 1$ and < 1000 are shown. For activation

of cellular compartments, the computation was the same, but the threshold for peak detection from the average curve was lowered to 0.1 and the threshold for activity maps was lowered to show pixels with $\Delta I/I > 0.1$ and < 500. Exponential decay time constants were determined from fitting single exponential functions to fluorescence *vs*. time traces (**Fig. 2, SI Appendix, Fig. S2**) using a custom Matlab code. 95% confidence intervals (CI) were converted to SEM using the following conversion: SEM = upper limit – lower limit of CI / 1.96.

Quantifying mechanical properties of cellular compartments. Mechanical properties of neurons were quantified using an AFM (BioScope Resolve, Bruker), mounted on the stage of an inverted optical microscope (LSM800, Carl Zeiss) and operated with the NanoScope 9.4R3 software (Bruker). The setup was isolated from noise, installed on a damping isolated table and placed in a noise-protected and temperature controlled chamber heated to 35°C. Neurons were plated (Materials and Methods, section 'neuron culture') on laminin-coated glass-bottom dishes (GWST-5040, WillCo Wells B.V.), and the dishes were placed on a baseplate heated to 37°C. Axons were labeled just before the experiments (Materials and Methods, section 'live cell staining'). Neurons were imaged with an optical system using a 10 mW 488 nm or 640 nm laser at 2 – 5% power, a 1 – 1.5 airy unit pinhole and a 63x water immersion lens (421787-9970-799 objective, NA 1.20, Carl Zeiss). Next, mechanical properties of neuronal axons, dendrites and somas were measured by operating the AFM in the force spectroscopy mode using paddle-shaped AFM cantilevers (PeakForce QNM – Live Cell, Bruker) having a nominal spring constant of 0.1 N m^{-1}, resonance frequency in fluid of 18 kHz, tip radius of 70 nm and tip half angle of 18°. Axons and dendrites were probed with 2 µm ramps and 100 pN force set point, while somas were probed with 4 – 6 µm ramps and 150 pN force set point. The tip velocity of 12 µm s^{-1} was kept constant for each measurement. The relative indentation depth for somas, axons and dendrites was kept at approximately 10% of their height. Experimental results are given from four separate neuronal preparations (**SI Appendix, Fig. S11**). Each neuron was probed on three subcellular compartments. Each data point shown is an average of three measurements, performed on distinct spots of an axon, dendrite or soma. The Poisson ratio of the cell was approximated to 0.5. To approximate the apparent Young's modulus, force-distance curves recorded on cellular compartments were fitted with a Sneddon Model (using the NanoScope Analysis 1.8 software).

Super-resolution microscopy. Stimulated emission depletion (STED) microscopy was performed using the STEDYCON (Abberior, Göttingen, Germany) head mounted onto a BX53 microscope body (Olympus, Hamburg, Germany.) and equipped with a UPlanSApo 100x/1.4 oil objective (Olympus). STED imaging following mechanical stimulation involved two microscopes, one for stimulation, one for super-resolution imaging. In order to identify the cells after transfer between microscopes, the neurons were cultured on gridded dishes (IBIDI, Gräfelfing, Germany, µ-Dish, 35 mm, high Grid-500). First, neurons were mechanically stimulated using AFM. After mechanical stimulation, the neurons were incubated for 1 h for any hallmarks of injury to develop, and then fixed for 5 min in 4% para formaldehyde (Ted Pella). Cells were washed 3x with PBS and then stained with anti-pan neurofascin primary antibody (clone A12/18, Neuromab) at 1:100 dilution for 1 h at RT on a shaker. Neurons were washed again 3x with PBS and stained with a secondary Alexa Fluor 594 - F(ab')2 - anti mouse antibody (Invitrogen) at 1:200 dilution in neurobasal medium and with phalloidin-STAR RED (Abberior) at a concentration of 1 unit ml^{-1} for 1 h at RT on a shaker. Finally, the fixed and stained neurons were washed 3x with PBS and mounted for imaging in the

STEDYCON In the STEDYCON, neurons were located using the gridded dish and imaged with excitation lasers at 595 nm (≈ 10 – 30% power for neurofascin-alexa 594) and 640 nm (≈ 5–20% power for phalloidin-STAR RED) and depletion laser at 775 nm (≈ 5% power). Using these settings, we achieved a resolution of ≈ 50 nm. Acquired images were processed in ImageJ (imagej.nih.gov/ij). Brightness and contrast were linearly adjusted for the entire image to compensate differences in fluorescence intensity. Line profiles of STED images of axon and dendrite were measured along 10 pixel wide lines using ImageJ.

Statistical analysis. Statistical analysis was performed using Prism 7 (GraphPad) as well as custom made Matlab scripts. Since we did not assume Gaussian distributions for all the data sets, we chose non-parametric two-tailed Mann-Whitney tests to compare two distributions (**SI Appendix, Figs. S2, S3, S4**). For statistical analysis of more than two distributions, we chose the non-parametric one-way ANOVA (Kruskal-Wallis) test (**SI Appendix, Figs. S2, S5, S11**). To statistically analyze datasets in which we scored three response types (no, transient and sustained response), we turned to the chi-square test for goodness of fit (**Figs. 3, 4, SI Appendix, Fig. S8**)**.** The chi-square test was performed by comparing the expected distribution against the observed distribution. This two-tailed test returned a p-value used to determine the statistical significance. Statistical analysis of experiments with large numbers of samples (**Fig. 5, SI Appendix, Fig. S10**) was performed using logistic regression relating treatment and time point to the variable $\Delta I/I$. We controlled for technical replicate and day of experiment to take into account non-treatment variation. We used model-based t-tests comparing the ratio of average response in $\Delta I/I$ at time point "post" to the average response in $\Delta I/I$ at time point "pre" within each treatment. p-values were calculated as a z-test with z-statistic = log(estimated OR)/SE(estimate) and assuming a two-sided test. We used a z-test rather than a t-test due to our large number of samples.

Supplementary Figures

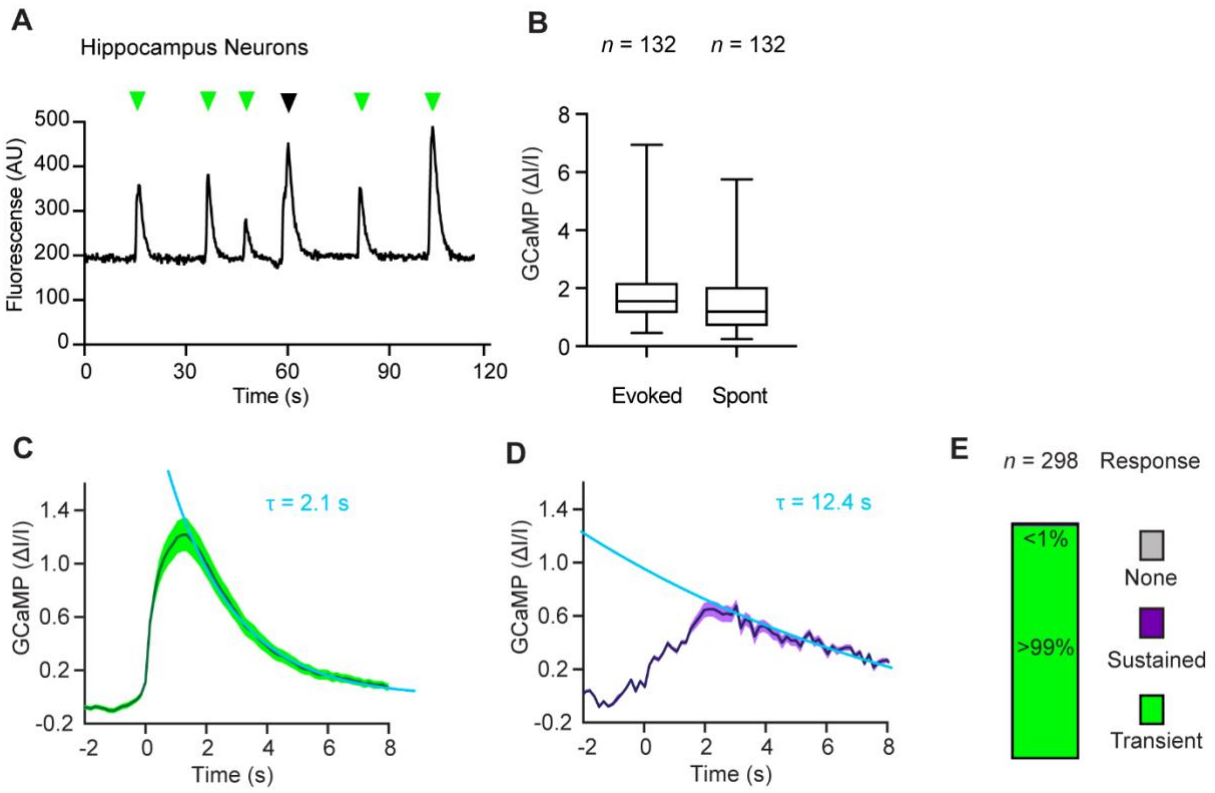

Fig. S1. Hippocampal neurons respond to shear stress. (A) Mean GCaMP6s signal (black) over time for a population of hippocampal neurons (*n* = 25) showing spontaneous responses (green arrowheads) and a mechanically evoked response (black arrowheads) to a single shear stress stimulation (3 s duration, 60 Hz). (B) Quantification from 3 independent experiments showing normalized GCaMP6S values for hippocampal neurons with evoked activity (left) and neurons with spontaneous activity (right). Boxes show mean, whiskers show min and max values. *n* represents the number of neurons analyzed. (C) Average fluorescence trace showing the transient GCaMP responses (*n* = 286) of hippocampal neurons (dark line, mean; shaded areas, SEM). The data was fitted by a single exponential function (light blue) to reveal the τ value. The transient responses show an exponential decay time constant τ = 2.1± 0.1 s (mean ± SEM). (D) Average fluorescence trace showing the sustained GCaMP responses (*n* = 3) of hippocampal neurons (dark line, mean; shaded areas, SEM). The data was fitted by a single exponential function (light blue) to reveal the τ value. The transient responses show a τ = 12.4± 3.5 s (mean ± SEM). (E) Percentage of hippocampal neurons not responding or showing a transient or sustained response. Height of bar and numbers both show percentages. *n* represents number of neurons analyzed.

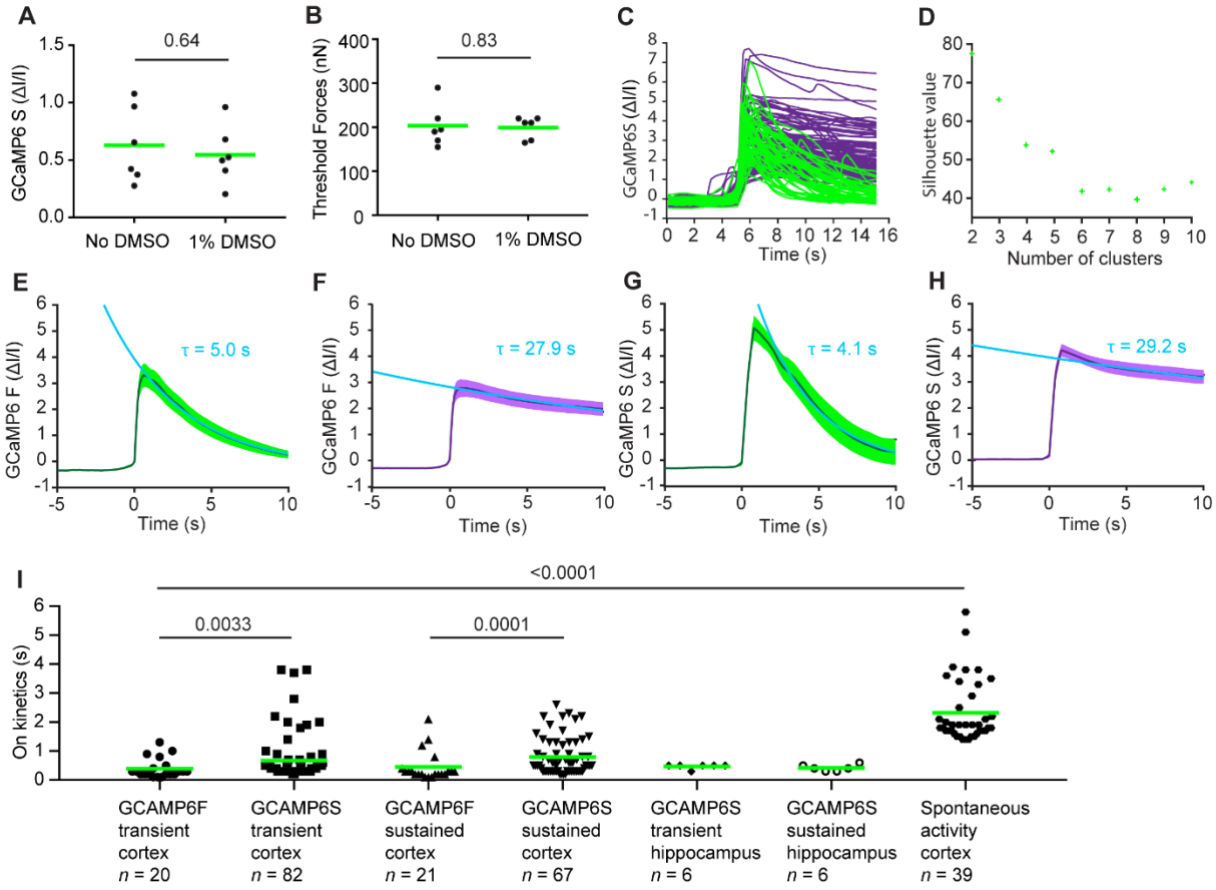

Fig. S2. Transient and sustained responses are independent of calcium sensor and neuronal cell type. (A and B) Normalized calcium signals (A) and threshold forces (B) for cortical neurons responding to soma stimulation pre (n = 6, left) and post (n = 6, right) addition of DMSO (1% vol/vol) to neurobasal media. Dots represent single cells, green bars mean values. Two-tailed Mann-Whitney tests were applied for statistical analysis. (C and D) Principal component analysis of cortical neurons being mechanically indented at the soma. **c,** Single-cell fluorescence responses (n = 143). Calcium levels were recorded using sensitive variant GCAMP6S. Purple traces cluster into a sustained population, green traces cluster into a transient population. The fluorescence traces were taken to calculate averaged traces in **Fig. 2e-d**, Principal component analysis (k-means) showing the probability for various numbers of clusters with two clusters scoring the highest (**Materials and Methods**). (E - H)**,** Average fluorescence traces showing the intracellular calcium level (GCAMP) of cortical (**e,f**) and hippocampal (G and H) neurons being mechanically indented at their soma (dark line, mean; shaded areas, SEM). Each trace was fitted with a single exponential function (blue line) to estimate the decay time τ of the calcium signal (given in mean ± SEM). (E) Transient responses recorded with fast variant GCaMP6F (n = 20). τ = 5.0 ± 0.1 s (mean ± SEM). (F) Sustained responses recorded with fast variant GCaMP6F (n = 21). τ = 27.9 ± 0.9 s. (G) Transient responses recorded with sensitive variant GCaMP6S (n = 6). τ = 4.1 ± 0.1 s. (H) Sustained responses recorded with sensitive variant GCaMP6S (n = 6). τ = 29.2 ± 0.5 s. (I) Rise time for GCaMP6F and GCaMP6S fluorescence signals in cortical and hippocampal neurons responding transient or sustained to the mechanical stimulation of their soma. For comparison, the rise time of the spontaneous activity is given for cortical neurons. The rise time (seconds) required for the calcium signal to increase from 20% to 90% of maximum fluorescence intensity is plotted. n represents number of neurons analyzed, dots represent single neurons, and green bars mean values. Two tailed unpaired Mann-Whitney tests were applied to determine statistical significance of two distributions, One-way ANOVA tests applied for statistical analysis of all distributions (****, P < 0.0001. F = 29.6).

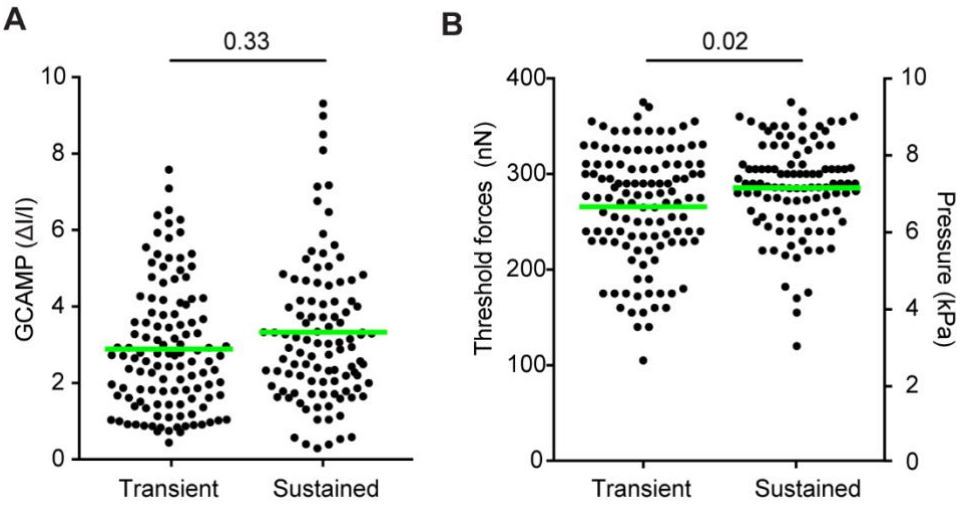

Fig. S3. The response of neurons to mechanical indentation of their soma differentiates force. (A and B) Normalized calcium signals (A) and threshold forces (B) for cortical neurons with transient (*n* = 119) and sustained (*n* = 105) responses to mechanical stimulation of the soma. Neurons were stimulated with force ramps from 50 – 400 nN. Dots represent single neurons, green bars the mean. Two tailed Mann-Whitney test, ns, *P* > 0.05; *, P < 0.05.

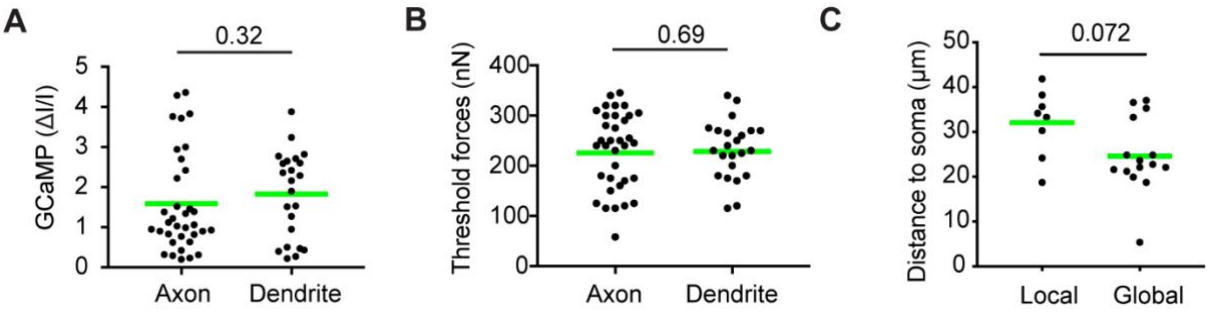

Fig. S4. Axons and dendrites show similar force thresholds and response peaks to mechanical stimulation. (A and B) Normalized GCaMP6S fluorescence intensity (A) and threshold forces (B) for cortical neurons responding to the mechanical stimulation of axon (*n* = 35) or dendrite (*n* = 23). (C) Local vs global responses of dendrites shown as a function of stimulus location. The more distant indentations evoked primarily local responses while indentations closer to the soma evoked mostly global responses (*n* = 23). Dots represent single neurons, green bars mean values. Two-tailed Mann-Whitney tests applied to determine statistical significance.

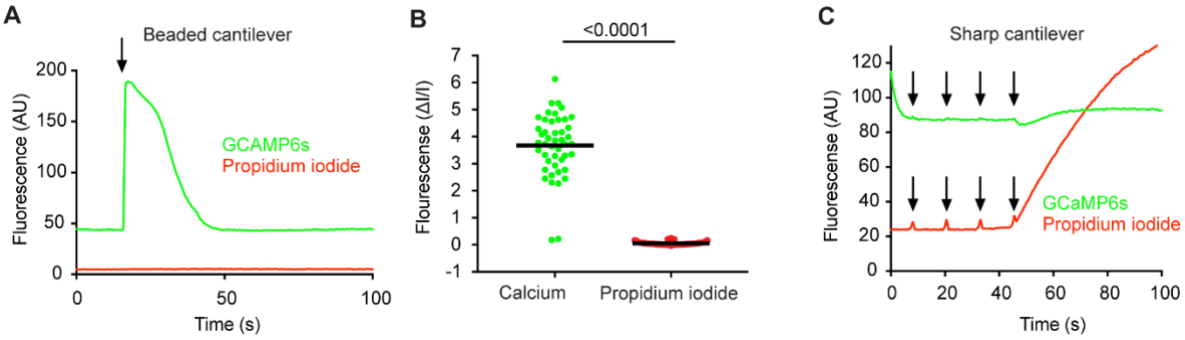

Fig. S5. Calcium entry of mechanically stimulated neurons is not mediated by membrane defects. (A) Time-lapse fluorescence of a single representative cortical neuron responding to soma indentation by a beaded cantilever. The calcium signal (GCaMP6S, green) responds to mechanical indentation (black arrow), while the intracellular propidium iodide signal (red) remains unchanged. (B) Normalized fluorescence (GCaMP6S, green and intracellular propidium iodide, red) of cortical neurons (n = 46) responding (transient and sustained) to mechanical stimulation of the soma. Dots represent single cells, black bars represent mean values. Two-tailed Mann-Whitney test was applied to determine statistical significance. (C) Positive control for (A) showing the disruption of the neuronal membrane indented by a sharp tipped cantilever. Time-lapse fluorescence of a single representative cortical neuron responding to soma indentation with a sharp tipped cantilever. Black arrows indicate, indentations of the cantilever tip into the neuronal membrane. The intracellular propidium iodide signal (red) shows loading of the dye while the GCaMP6S (green) remains mostly unchanged. Experiment repeated 8 times.

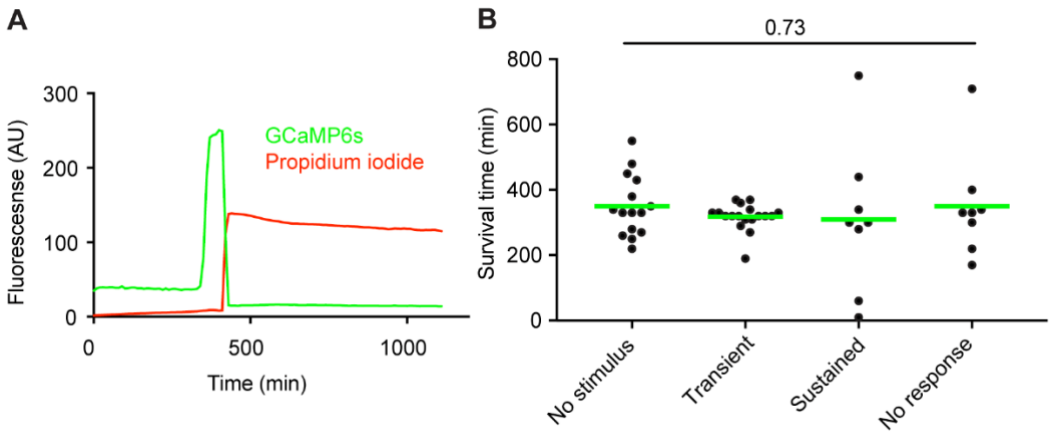

Fig. S6. Mechanically stimulated neurons do not show hallmarks of cell death. (A) Plot showing long term fluorescence of a single non-stimulated cortical neuron imaged for 20 h (1 fluorescence image recorded every 10 min). The sudden increases in calcium measured by the GCaMP6S signal (green) at 360 min and uptake of propidium iodide (red) at 420 min are used as a proxy for cell death. Until this inflection points, cells are surviving. (B) Survival time of non-stimulated cortical neurons and neurons with soma stimulation. The GCaMP signal (see A) was used to determine the type of response to mechanical stimulation and the survival time. Survival times are plotted for non-stimulated cortical neurons ($n = 15$) and for mechanically stimulated cortical neurons showing a transient ($n = 18$), sustained ($n = 8$) or no ($n = 8$) calcium response. Dots represent single neurons, green bars mean values, and n the number of neurons analyzed. One-way ANOVA tests were applied for statistical analysis (ns, $P > 0.05$, $F = 0.3$).

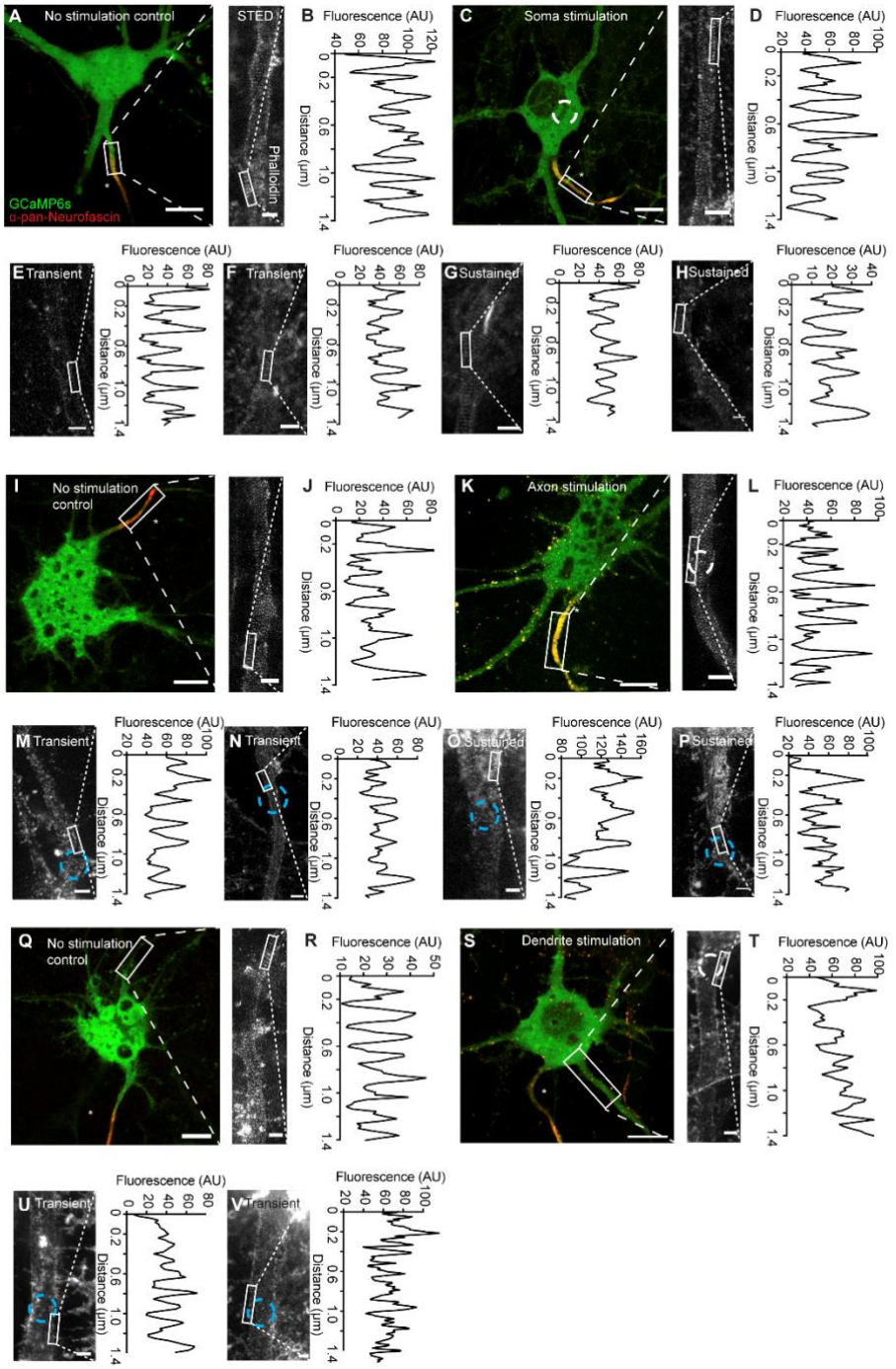

Fig. S7. Super-resolution microscopy reveals cytoskeletal integrity of mechanically stimulated cortical neurons. Confocal microscopy of GCaMP6S (green) and Axon initial segment (red). Inlays show stimulated emission depletion (STED) microscopy of stained actin cytoskeleton (grayscale) of cortical neurons without (A and L and Q) and with (C and K and S) mechanical stimulation. GCaMP6S (green) expressing cortical neurons were mechanically stimulated, fixed and stained with anti- alpha-pan neurofascin Alexa fluor 594 (red) and STAR RED phalloidin (white). Axons are marked with asterisks, and sites of stimulation are indicated with dashed circles. Scale bars of confocal images, 10 µm and of STED images, 1 µm. (E – H**),** STED images and fluorescence intensity profiles corresponding to the white box in the STED inlays for neurons after soma stimulation. (M - P), STED images and fluorescence intensity profiles corresponding to the white box in the STED inlays for neurons after axon stimulation. (U and V) STED images and fluorescence intensity profiles corresponding to the white box in the STED inlays for neurons after dendrite stimulation.

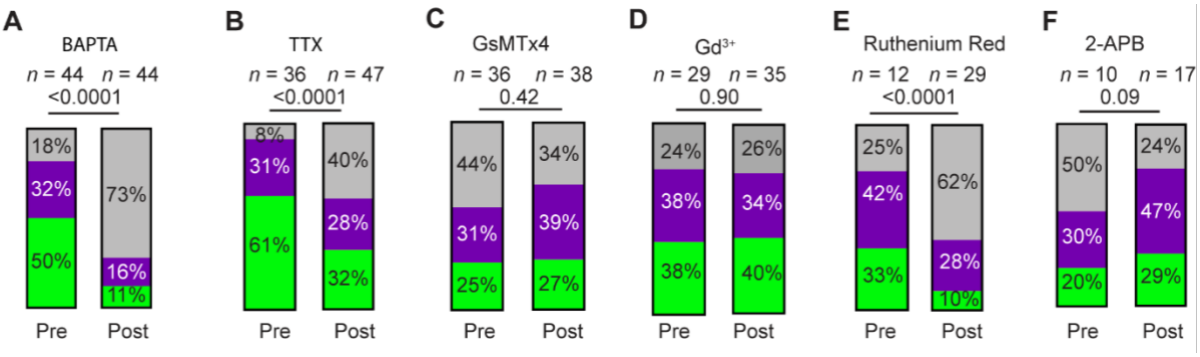

Fig. S8. Chemical compounds effect calcium responses in cortex neurons stimulated by soma indentation. Responses of cortical neurons stimulated by AFM soma indentation before (left) and after (right) addition of chemical compounds. Bar graphs show percentage of neurons with no response (grey), sustained response (purple) and transient response (green). Number of neurons tested are indicated above the bars. Chi-square test was used for statistical analysis. (A) Extracellular calcium chelator BAPTA free acid (2 mM). (B) Voltage-gated sodium channel inhibitor TTX (1 µM). (C) Mechanosensitive channel inhibitor GsMTx4 (2.5 µM). (D) Stretch activated channel inhibitor gadolinium chloride (Gd_{3+}, 100 µM). (E) Non-specific ion channel inhibitor ruthenium red (100 µM). (F) Effect of the mechanosensitive channel inhibitor 2-APB (100 µM).

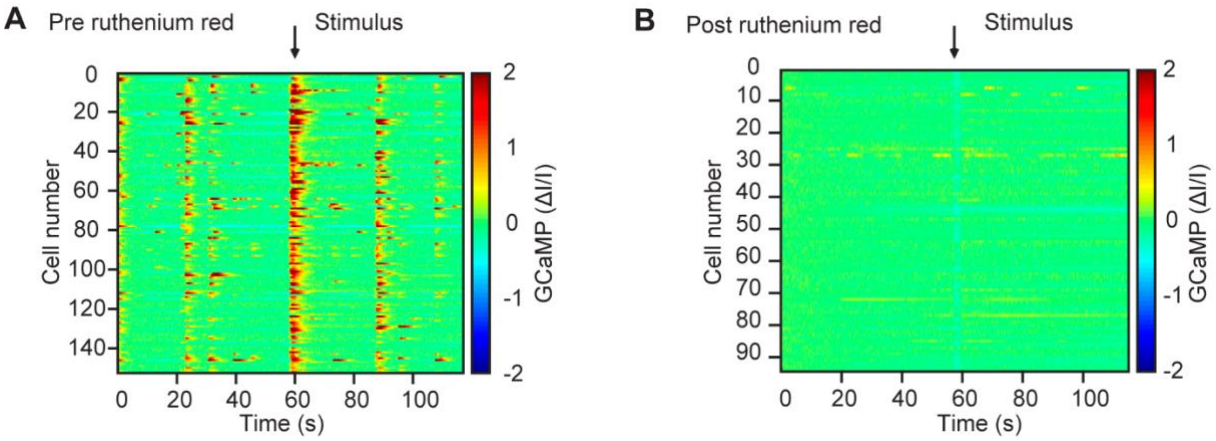

Fig. S9. Visualization of how chemical compounds effect calcium responses in cortex neurons stimulated by shear stress. (A and B) Raw GCaMP6s fluorescence traces of the same set of cortical neurons mechanically stimulated by pistons before (A, left, *n* = 149) and after (B, right, *n* = 93) the addition of chemical compound ruthenium red (100 µM) to perturb channel activity. Heat map color coding represents the magnitude of the GCaMP6S signal. Time of stimulus is indicated by the black arrow (top).

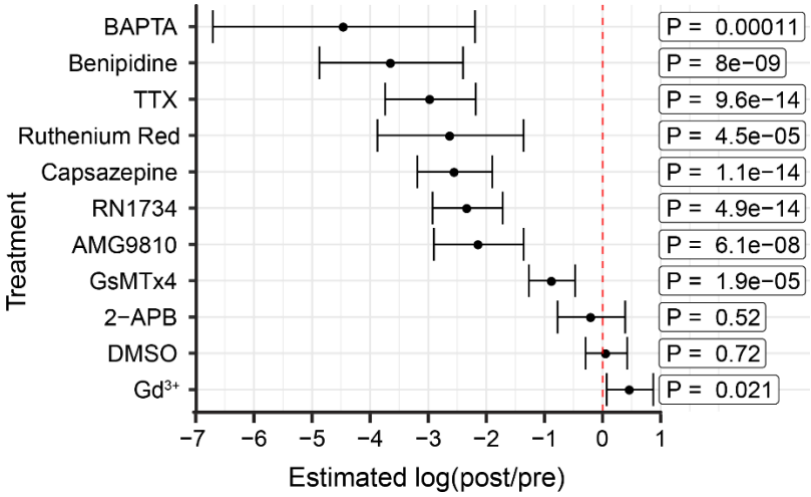

Fig. S10. Logistic regression comparing the effect of various chemical compounds to neuronal responses evoked by shear stress. Comparison of chemical compounds used in **Fig. 5**. The logistic regression model **(SI Appendix, Materials and Methods)** was applied to compute the ratio of average calcium response values pre and post treatment with various compounds. Black dots: mean, error bars: 95% confidence intervals. P-values for each treatment group are given on the right. Red line: pre = post. For all data on the left side of the red line the chemical treatment inhibited mechanically evoked responses, for data on the right side of the red line the chemical treatment potentiated mechanically evoked responses.

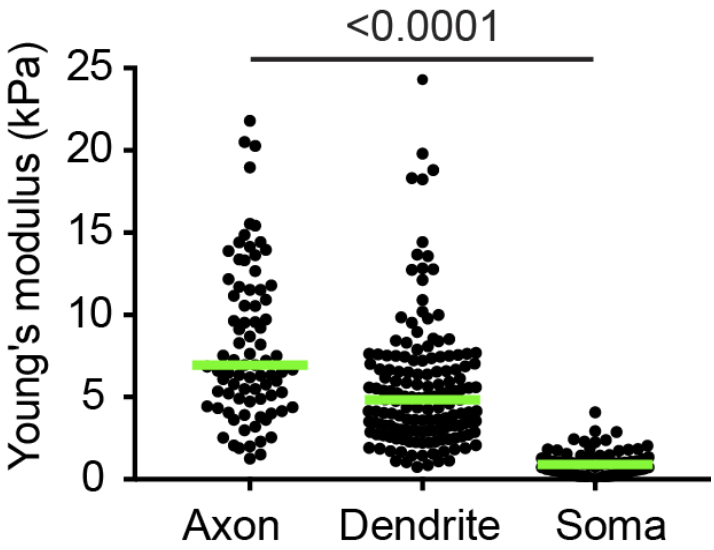

Fig. S11. Mechanical properties of neuronal compartments. Apparent Young's modulus of compartments of cortical neurons measured by AFM. Elastic moduli of axon (n = 85), dendrite (n = 153) and soma (n = 84) of cortical neurons aged 2 – 17 days in vitro (DIV). n represents the number of independent measurements. One-way ANOVA test was applied to determine statistical significance (****, P < 0.0001, F = 84.5).

Supplementary Tables

Table S1. mRNA transcript levels of ion channels in E18 and adult cortical rat neurons.

	Ion channel	TPM in E18 forebrain	TPM in adult brain	Reference
1.	TRPV1	0.7	1	(6), (7)
2	TRPV4	1.0	Not available	(6), (7)
3.	TRPC1	9.0	19	(6), (7)
4.	TRPC5	5.0	12	(6), (7)
5.	Piezo 1	Not available	0.8	(7)
6.	TTX sensitive Na_V 1.2	Not available	112	(7)
7.	TTX sensitive Na_V 1.3	Not available	23	(7)
8.	Bendipidine sensitive Ca_V (L-type / T-type Ca_V)	Not available	Not available	Not available

Table S1. mRNA transcript levels of ion channels relevant to our chemical inhibition experiments. Transcript levels are reported as transcripts per million (TPM) in embryonic E18 rat forebrain and adult brain.

Supplementary References

1. M. Radivojevic *et al.*, Tracking individual action potentials throughout mammalian axonal arbors. *Elife* **6** (2017).
2. J. Xu *et al.*, GPR68 Senses Flow and Is Essential for Vascular Physiology. *Cell* **173**, 762-775 e716 (2018).
3. S. S. Ranade *et al.*, Piezo1, a mechanically activated ion channel, is required for vascular development in mice. *Proc Natl Acad Sci U S A* **111**, 10347-10352 (2014).
4. D. Martinez-Martin *et al.*, Inertial picobalance reveals fast mass fluctuations in mammalian cells. *Nature* **550**, 500-505 (2017).
5. J. L. Hutter, J. Bechhoefer, Calibration of atomic-force microscope tips. *Rev Sci Instrum* **64**, 1868-1873 (1993).
6. E-MTAB-6811 - Rat RNA-seq time-series of the development of seven major organs. *https://www.ebi.ac.uk/arrayexpress/experiments/E-MTAB-6811/* (2015).
7. Y. Yu *et al.*, A rat RNA-Seq transcriptomic BodyMap across 11 organs and 4 developmental stages. *Nat Commun* **5**, 3230 (2014).

Legends for Supplementary Videos

Video S1. Ensemble measurements of mechanically stimulated neurons. Time-lapse wide-field fluorescence images of cortical neurons expressing GCaMP6S showing the baseline fluorescence, mechanically evoked response (stimulus indicated by text label, top left corner), return to baseline and spontaneous response in the absence of mechanical stimulation. The images were recorded while applying shear stress as described (**Fig. 1**).

Video S2. Transient response to the mechanical stimulation of a soma. Time-lapse confocal fluorescence images of cortical neurons expressing GCaMP6S showing the baseline fluorescence, transient response to mechanical stimulation and return to baseline. The images were recorded while applying soma indentation by AFM as described (**Fig. 2**).

Video S3. Sustained response to the mechanical stimulation of a soma. Time-lapse confocal fluorescence images of cortical neurons expressing GCaMP6S showing the baseline fluorescence and sustained response to mechanical stimulation without return to baseline fluorescence. The images were recorded while applying soma indentation by AFM as described (**Fig. 2**).

Video S4. Global response to the mechanical stimulation of an axon. Time-lapse confocal fluorescence images of cortical neurons expressing GCaMP6S showing the baseline fluorescence, transient response to mechanical stimulation and return to baseline. The images were recorded while applying axon indentation by AFM as described (**Fig. 4**).

Video S5. Local response to the mechanical stimulation of a dendrite. Time-lapse confocal fluorescence images of cortical neurons expressing GCaMP6S showing the baseline fluorescence, transient response to mechanical stimulation and return to baseline. The images were recorded while applying dendrite indentation by AFM as described (**Fig. 4**).